RSC Advances

RSC Publishing

PAPER

View Article Online
View Journal | View Issue



Cite this: *RSC Adv.*, 2013, **3**, 25997

# Substrate binding to *Candida tenuis* xylose reductase during catalysis

Michael Vogl and Lothar Brecker*

Received 25th March 2013
Accepted 4th October 2013

DOI: 10.1039/c3ra41448e

**www.rsc.org/advances**

*Candida tenuis* xylose reductase (*Ct*XR) is studied by *in situ* NMR, saturation transfer difference (STD) NMR, and molecular docking with respect to its substrate and coenzyme binding in ternary complexes. The natural substrate Xyl as well as Glc and methyl-glucosides preferentially bind as α-anomers of the pyranose forms. These α-anomers are transformed faster, predominately leading to STD effects in the formed products, and can be better docked into the *Ct*XR active site than the β-anomer. The reduction is initiated by α-Xyl*p* ring opening prior to hydride transfer from NADH. Binding and transformation of unnatural 2,4-dichloroacetophenone is not as good, although it is reduced with very high catalytic efficiency. STD NMR indicates a reasonable amount to leave the ternary complex in unreduced form. The molecular docking calculation confirms this result, as only a couple of the investigated ternary complexes allow reduction of the substrates.

## Introduction

Enzymes are biological catalysts used in many different synthetic applications. In particular oxidoreductases [E.C.1.1.1] are often applied for this purpose.[1–3] Their high transformation rates as well as the asymmetric induction in formation of highly enantiomeric enriched secondary alcohols cause a growing awareness of this enzyme group.[3–6] Additionally, several oxidoreductases do not only transform their natural substrates, but also bind and process artificial compounds with high transformation rates.[7,8] Hence, there is a growing interest to investigate details of the enzymatic mechanism. Especially, comprehensive knowledge of substrate accommodation in the binding pocket helps to understand the acceptance of unnatural substrates and guides rational design of enzyme variants with altered substrate specificities.[9,10]

Many different methods have been established during the last decades to gain insight into ligand binding for different enzyme systems.[11] In particular, *in situ* $^1$H NMR and Saturation Transfer Difference (STD) NMR are well established to study product formation and ligand enzyme binding processes, respectively.[11–17] In these techniques the substrates and products are monitored and provide direct information about their interaction with the active site and surrounding areas of the enzyme. Furthermore, data gained by these methods can be visualized and refined using *in silico* docking methods.[18]

In the present study xylose reductase [E.C.1.1.1.21; D-xylose reductase] from the yeast *Candida tenuis* (*Ct*XR) is investigated. Its natural substrate xylose is reduced by this enzyme to the corresponding xylitol with concomitant oxidation of NADPH or NADH to $NADP^+$ or $NAD^+$, respectively.[19–21] The different anomeric forms of xylose in the natural aqueous environment complicated a detailed binding analysis so far. Additionally, many non-natural substrates are quite well accepted by *Ct*XR. In particular, mono- and di-chloro-substituted acetophenones are transformed to the corresponding phenyl ethanols with very high transformation rates.[22,23] Hence, 2,4-dichloroacetophenone is used as non-natural model substrate for complementary binding studies. The corresponding results from NMR experiments and docking calculations provide a better understanding of *Ct*XR substrate specificity in order to make direct mutations in future.

## Results and discussion

### Binding of different xylose anomeric forms

The natural substrate xylose is reported to be reduced by *Ct*XR as aldehyde in its open chain form.[19,20,24] This result, determined from kinetic investigations, is in good agreement with the common mechanism of oxidoreductase catalyzed carbonyl reductions using NADH. We now study the dynamic procedure of substrate binding by *in situ* NMR and monitor the concentrations of the two different Xyl*p* anomers during transformation. At 303 K, customary used for previous investigations, α- and β-anomer amounts decreased in the same ratio using 0.36 μM *Ct*XR.[14] However, lowering the temperature to 283 K and using 7.2 μM *Ct*XR, the α-anomer is consumed considerably faster (Fig. 1(a)). This change is caused by a distinctly reduced anomerization rate, while the reaction rate of the *Ct*XR catalyzed reaction is not as intensively influenced by the 20 K temperature decrease, in particular due to the larger *Ct*XR concentration.[25,26] The anomerisation of xylose at 283 K is,

*University of Vienna, Institute of Organic Chemistry, Währinger Straße 38, A-1090 Wien, Austria. E-mail: lothar.brecker@univie.ac.at*

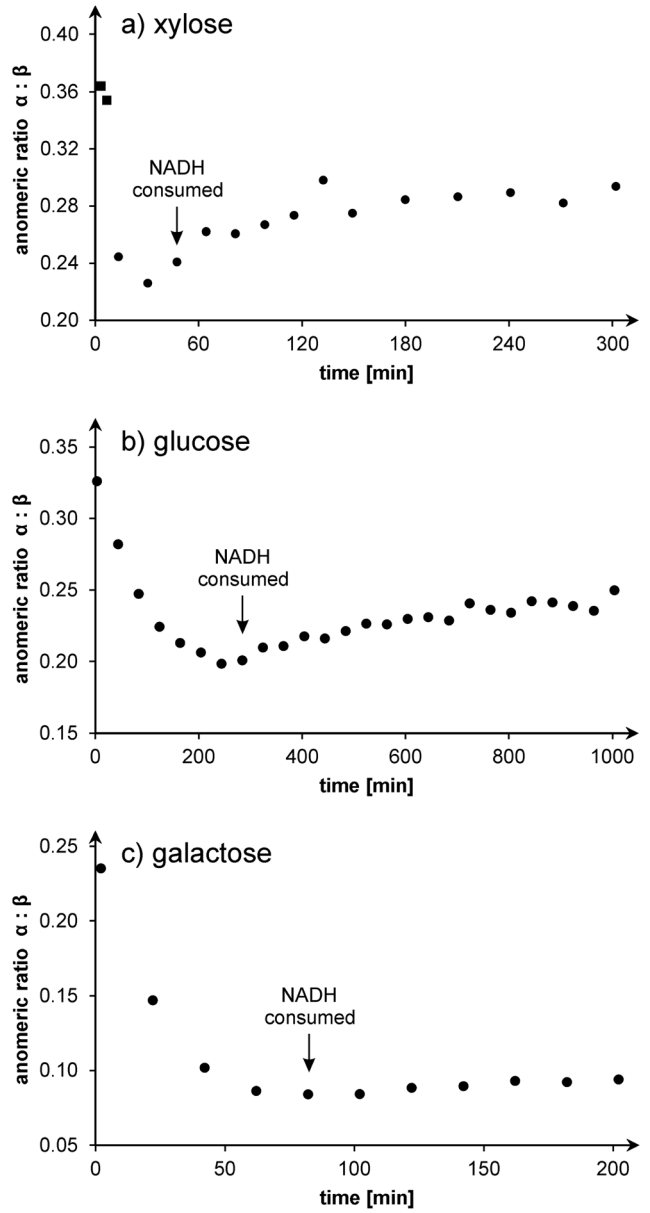


**Fig. 1** α- and β-anomeric ratio of the substrates xylose (a), glucose (b), and galactose (c) during *Ct*XR catalyzed reduction at 283 K. Starting concentrations of carbohydrates, NADH, and *Ct*XR were 1.5 mM, 0.5 mM, and 10.3 μM, respectively. Anomeric ratios during reactions have been determined by *in situ* NMR monitoring all proton signals which were not overlapping. An average value of all integrals belonging to one compound has been made. Only the initial ratio of xylose anomers (indicated by squares) has been determined prior to addition of the enzyme and from a preliminary measurement after enzyme addition, as quite fast reaction did not allow the determination of accurate starting point during transformation. Reduction of the α-anomer is obviously faster in all three cases resulting in a growing excess of the β-anomer during reaction. Then anomerization results in the equilibrium. The equilibrium at the end differs from the starting point, as presence of *Ct*XR causes mainly α-Xyl binding and ring opening. This leads to an increase in ring opening and release of the α-anomer compared to the β-anomer. The released aldehyde, however, rearranges to the two anomeric forms without any influence from the *Ct*XR. Consequently the dynamic equilibrium shifts to a higher amount of β-anomer compared to the starting point. Addition of *Ct*XR solutions did not cause changes of any other parameters like temperature, pD,[32] or ion concentration in reasonable amount, as all $^1$H NMR shifts remained constant.

hence, not fast enough to completely compensate concentration changes of α- and β-Xyl*p* caused by a preferred *Ct*XR reduction of the α-Xyl*p*. This anomer is obviously preferentially bound at the active site and isomerized to the open chain aldehyde form during the binding process. Therefore, the xylose α-anomer is mainly reduced to xylitol. The amount of α-xylose, which is considerable longer bound to *Ct*XR is considerable low. This caused by the Xyl : *Ct*XR binding which has a $K_m$ of 91 mM and by the molar ratio of the two compounds, which is 150 : 1. Having NADH in deficient proportion, the reduction stops after its complete oxidation to $NAD^+$ and the α- to β-Xyl*p* anomeric ratio slowly recovers to the dynamic equilibrium (Fig. 1(a)).

The final α- to β-anomeric ratio of Xyl in presence of *Ct*XR is slightly smaller than in absence of the enzyme at the start of the reaction. This difference is likely also caused by preferred binding of the α-anomer, which is then opened to the aldehyde form but not reduced due to lack of NADH. Release of the not transformed aldehyde from the Xyl/*Ct*XR and Xyl/*Ct*XR/$NAD^+$ complexes lead to formation of both α- to β-anomeric forms. Consequently to an access of the β-form is generated in comparison to the equilibrium at the starting point.

Performing this *in situ* NMR experiment at 283 K with the also accepted aldoses glucose, galactose, and arabinose provides very similar results. The α-anomers are always preferentially bound, isomerized, and reduced (Fig. 1(b) and (c)). Best accepted unnatural substrate, 2,4-dichloroacetophenone is transformed by *Ct*XR with a catalytic efficiency of 1128 $mol^{-1}$ $s^{-1}$. Taking into account that *Ct*XR predominantly binds the α-Xyl for reduction, the unnatural substrate 2,4-dichloroacetophenone is accepted better.[23,27] However, xylose would have been transformed with higher catalytic efficiency, if it had only been bound and accepted in the low aldehyde concentration. Hence, comparison of these natural and unnatural substrates is now made, with particular focus on their binding.

### STD NMR of ternary ligand/coenzyme/*Ct*XR complexes

The STD NMR technique is a well suited method to investigate ligand protein interactions. Its principle is to measure the magnetization which is transferred by dipole–dipole interaction from the protein to the protons of a non covalently bound ligand. This method was developed to study binding of single ligands and mixtures to receptor-proteins.[11,12,28,29] However, STD NMR can also be used to study ligand enzyme interactions.[14,15] Apart from binding of substrates, inhibitors, and products, the binding behavior during the catalytic event can also be studied.

In coenzyme depending transformations, however, ternary substrate/coenzyme/enzyme complexes are formed during the reactions and both, substrates and coenzymes are structurally modified at the same time. The resulting reaction mixtures make binding investigations rather complex, as apart from the productive complexes other binary and ternary complexes are formed. They all likely possess slightly different conformations, which cause different signal intensities in the STD spectra. However, some of these versatile complexes can be neglected as the products and transformed coenzymes are only present in very small concentrations at the beginning or end of an investigated reaction

 

(Fig. 2). Suitable short measurement times therefore allow to record *in situ* STD NMR spectra, which provide detailed information about binding at different stages of the reaction process. Furthermore, detailed reference STD spectra can be recorded from binary and ternary complexes, which do not lead to substrate transformations. In such experiments binding times can be roughly estimated in particular from STD signal intensities, which are diminished by reasonably short or long binding times.[12,14,15]

### STD NMR of ternary Xyl/NADH/*Ct*XR complexes

Based on the *in situ* NMR experiments and preliminary STD NMR investigations of *Ct*XR catalyzed transformations, a detailed binding analysis is performed.[14] Monitoring the binary mixture of the enzyme (0.51 μM) and xylose (6.7 mM) not leading to transformation due to lack of the coenzyme provides very small STD signals from both xylose anomers (Fig. 3(a), Table 1(a)). The average STD signal intensities are in good agreement with the *ca.* 1 : 2 ratio of the anomers in aqueous solution. Both anomers are therefore bound and released in similar amounts. There is no evidence that Xyl undergoes a temporary rearrangement to the open chain aldehyde form during the binding period, when no NADH is present in the active site and hence no transformation occurs.

Hence, in the next step NADH was added as coenzyme (7.5 mM) to study substrate binding during the xylose reduction. The gained results are in good agreement with earlier reported data and support this investigation.[14] Here the STD-signals of the α-anomer protons decrease distinctly and only the signals from the β-anomer are left as shown in Fig. 3(b). The α-Xyl binds in the ternary complex, gets magnetized, and is completely reduced to xylitol. Then it leaves the enzyme as magnetized product xylitol and causes STD signals of this product. Due to symmetry of xylitol no detailed assignment to single protons is possible. The concentration of the magnetized α-anomer in the solution is low and causes only small STD signals, as only a small amount is released as unreacted xylose from the complex. On the other hand, the β-anomer obviously binds in the ternary complex and takes over magnetization from the protein. Then it is released without ring opening leading to the aldehyde.

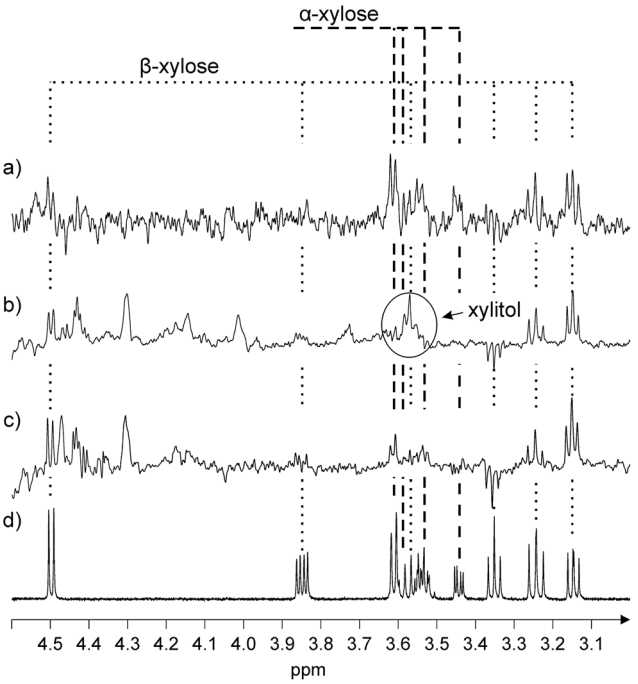


**Fig. 3** Cutout of STD NMR spectra recorded from (a) Xyl/*Ct*XR, (b) Xyl/NADH/*Ct*XR, and (c) Xyl/$NAD^+$/*Ct*XR, as well as of (d) $^1$H NMR spectrum of Xyl for comparison. Shown are all proton signals of both Xyl anomers, except the H-1 signal of α-Xyl. (a) STD effects of xylose binding to *Ct*XR in a binary complex are reasonable small and indicate that both Xyl anomers likely bind to the enzyme with quite short binding times.[13,28] (b) In the productive Xyl/NADH/*Ct*XR complex STD effects of β-Xyl are quite distinctive, while α-Xyl is not released from the *Ct*XR, but transformed to xylitol. Release of this product causes STD signals between 3.5 and 3.7 ppm indicated in a circle.[15] Further STD signals belong to NADH protons. (c) In the unproductive Xyl/$NAD^+$/*Ct*XR complex STD NMR signals are distinctly smaller and indicate both anomers to be bound and released from the enzyme. These data portent a spatially close binding of substrate and coenzyme to *Ct*XR. Phase error of H-4 from β-Xyl at *ca.* 3.45 ppm is likely caused by an effect discussed earlier and based on interference with $D_2O$ irradiated by the lock frequence.[14]

However, it cannot be excluded that a small amount of β-Xyl is also opened and reduced to xylitol, because the substrate conformer cannot be identified from the symmetrical product. STD effects of xylose anomers are listed in Table 1(b).

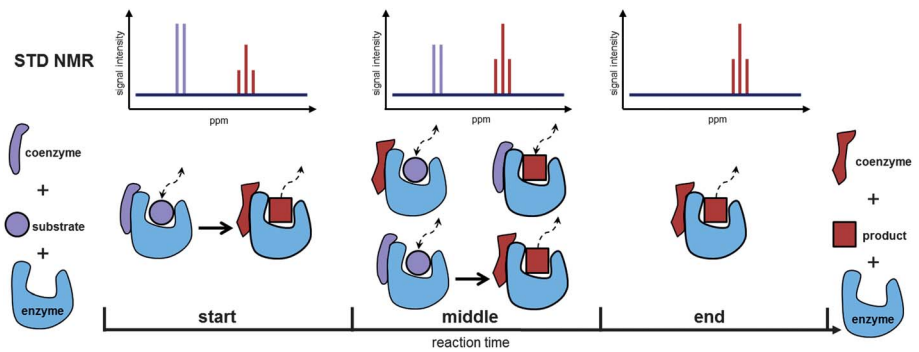


**Fig. 2** Schematic progress of *in situ* STD NMR measurements considering binding of substrates and products. At the start of the reaction bound substrate and first generated product are released from the enzyme showing STD effects. In the middle of the reaction having a mixture of substrate, product, and both forms of the cosubstrate also unproductive binding is possible. The different ternary complexes lead to average STD signals of substrates and products. At the end of the reaction only the product and the transformed form of the cosubstrate are present, leading to STD signals caused by this ternary complex.

**Table 1** STD NMR effects of xylose anomers and of glucopyranosid anomers binding to *Ct*XR in binary as well as in ternary complexes with NADH. All spectra are referenced to 100% for the largest STD effect in the measurement. Comparison between STD effects of the spectra can be estimated from signal to noise ratios. Long substrate/product binding times leading also to small STD effects can be excluded[13,14]

| Substrate | H-1 | H-2 | H-3 | H-4 | H-5a | H-5b | H-6a | H-6b | $CH_3$[b] |
|---|---|---|---|---|---|---|---|---|---|
| **(a) *S/N* = ~10** | | | | | | | | | |
| α-Xylose | 20 | 50 | 30 | 35 | 25 | 25 | — | — | — |
| β-Xylose | 50 | 100 | 40 | 30 | 20 | 80 | — | — | — |
| **(b) *S/N* = ~19** | | | | | | | | | |
| α-Xylose/NADH[c] | 10 | 10 | 15 | 15 | 20 | 10 | — | — | — |
| β-Xylose/NADH | 70 | 100 | 45 | 20 | 70 | 45 | — | — | — |
| **(c) *S/N* = ~12** | | | | | | | | | |
| α-Glucopyranosid | nd[d] | 100 | 90 | 40 | 90 | — | 50 | 70 | 60 |
| β-Glucopyranosid | 30 | 100 | 30 | 60 | 60 | — | 30 | −30[a] | 60 |
| **(d) *S/N* = ~15** | | | | | | | | | |
| α-Glucopyranosid/NADH | nd[d] | 100 | 90 | 40 | 90 | — | 50 | 60 | 60 |
| β-Glucopyranosid/NADH | −30[a] | 100 | 40 | 60 | 60 | — | 40 | 40 | 70 |

[a] Phase error are likely caused by an effect discussed earlier and based on interference with $D_2O$ irradiated by the lock frequence.[14] [b] Value refers to all three proton of the methyl group. [c] Partly overlapped from xylitol signals (see Fig. 3). [d] Not determined due to overlap with impurities.

The higher intensities of STD signals from xylose compared to those from xylitol might be explained by a slightly longer binding time of the unreduced β-Xyl. Such faster release of xylitol is explicable by the necessity of the enzyme to be ready for the next binding process of xylose. However, STD signal intensity might also be caused by a faster release of more β-Xyl molecules, which is however not in accordance to Xyl : *Ct*XR binding having a reasonable low $K_m$ of 91 mM. Hence, the biocatalyst is quite likely optimized to release the product faster than the untransformed substrate. The transferred magnetization during the STD measurement is therefore larger in case of β-Xyl. However, the binding time of β-Xyl is obviously not long enough to compensate for this effect.[12,28]

### STD NMR of ternary *O*-methyl-Glc*p*/NADH/*Ct*XR complexes

In another approach a modification of the substrate is made in order to mimic productive ternary complexes, however, without leading to the reaction. For that propose we used *O*-methyl-glucosides, an analogue of the substrate Glc.[24] These substrate analogues do not undergo anomerization and cannot be opened to the aldehyde form. Therefore, in binding studies the resulting ternary complex is similar to those that are present at the beginning of the Glc or Xyl reduction processes.

Analyzing the two binary complexes of anomeric *O*-methyl glycosides (6.5 mM) and *Ct*XR (0.51 μM), the *O*-methyl-α-Glc*p* protons show on average higher STD intensities compared to those of *O*-methyl-β-Glc*p*. Only protons H-2 of both anomers have the same intensities and the proton H-4 of the β-anomer possess larger intensities than the corresponding protons from *O*-methyl-α-Glc*p* (Table 1(c)). Hence, the α-anomer obviously takes over a larger amount of magnetization than the *O*-methyl-β-Glc. This greater dipole–dipole interaction is likely caused by higher $k_{on}$ and $k_{off}$ rates and a better fit of the *O*-methyl-α-Glc*p* to the *Ct*XR binding side, which leads to optimal proximity of the binding partners. The release is, however, still fast enough and not resulting in a decrease of the STD signal intensity, which might be caused by longer binding times. The average $K_D$ values of all investigated carbohydrates are in the mM range being by far optimal for the generation of STD signals.[11]

The corresponding anomerically pure ternary Me-Glc*p*/NADH/*Ct*XR complexes have been studied with further STD NMR measurements. In comparison of the two anomers, the STD signals indicate that the *O*-methyl-α-glucoside again shows larger STD-effects than the β-anomer. However, the difference is not as distinct as in the absence of NADH (Table 1(d)).

In comparison to the STD effects of the free xylopyranose, there are significant consistencies. The protons of β-Xyl*p* and of *O*-methyl-β-Glc*p* show a very similar binding pattern. Hence, the binding of the two substrate analogues can be assumed to be quite similar to those of the xylopyranoses at the beginning in the productive transformation.

### Docking and simulation of Xyl/NADH/*Ct*XR complexes

A molecular docking of substrates to the binary complex can be made by an *in silico* technique on basis of the previously published structure of a co-crystallized *Ct*XR/$NAD^+$ complex.[30] It allows an illustration of the ternary complex. For this purpose, a simulation of the *Ct*XR/NADH complex is made, which is based on the *Ct*XR/$NAD^+$ crystal structure (PDB-entry 1MI3, http://www.rcsb.org). Such approximation is possible, as the STD effects are very similar for both complexes. Based on this structure a comparison of molecular modeling and NMR based results is made.

Molecular docking of β-xylose shows that this anomer is preferentially bound in two regions next to the active side. One of these areas is approximately 4 Å away from the transferrable hydride of NADH. Additionally, Tyr-51 and His-113, which are supposed to be involved in stabilizing the open from of the

 

aldehyde,[31] are placed in a distance of about 2.5 Å. Such spatial location does neither allow a rearrangement, nor a hydride transfer (Fig. 4(a)). However, it is close enough to the protein to absorb magnetization *via* dipole–dipole interaction, causing STD signals. The measured STD signal intensities are in good accordance to the special closeness between substrate protons and protons from the protein. The second area is on the opposite side of NADH, which is also more than 5.0 Å away from the transferrable hydride. Additionally, the important amino acids are not in this area (Fig. 4(b)). Hence, β-xylose does not fit well into the active site and is not reduced. The only possibility to enable the hydride transfer is a non *Ct*XR influenced anomerization in this position, resulting in the α-anomer.

The α-xylose, however, fits perfectly into the reactive site close to NADH. The *pro*-R hydrogen is in hydride-transfer distance of *ca.* 1.82 Å away from the carbon of the hemiacetal function, which forms the aldehyde in the rearrangement. Furthermore, STD data are also in good agreement with this ternary complex conformation, especially as the α-Xyl protons showing large STD effects are spatially close to the *Ct*XR protons. The distances to the nearest amino acids protons of Tyr-51 is between 2.0 Å and 2.6 Å and the one to protons of His-113 is 3.6 Å (Fig. 4(c)).

The results of such simple docking experiments should be treated carefully in general. The flexible loop region of the *Ct*XR is involved in substrate binding and its movability is most likely responsible for the large substrate acceptance of the enzyme.[31] In the used docking calculation, however, only the ligand structure is optimized *in silico* while the enzyme is kept rigid. However, the present results are in excellent agreement with the *in situ* NMR and, in particular, with the STD NMR. It can hence be concluded that the results from docking visualize a correct binding and indicate a preferential binding and use of α-xylose prior to ring opening and reduction.

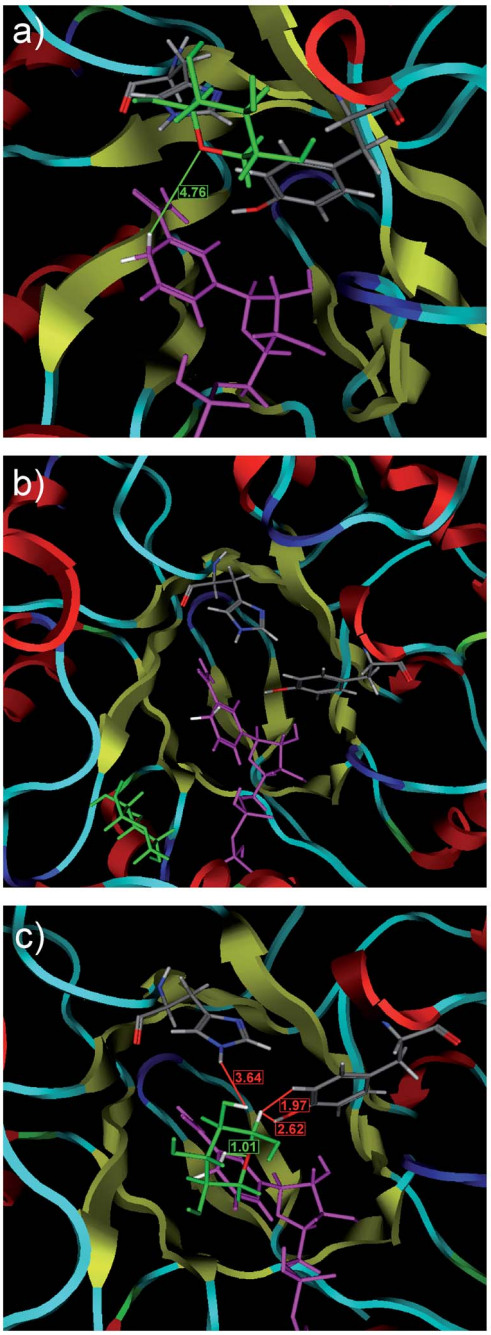


**Fig. 4** Molecular docking of xylose to a complex of NADH and *Ct*XR.[18] The xylose anomers are shown in green, while the NADH is visualized in pink. A couple of indicative distances between atoms are shown in red ($^1$H–$^1$H distances, responsible for STD effects) and green (indicative distances between xylose, NADH, and *Ct*XR). All are indicated with the length given in Å. Docking of β-xylose results in two different orientations shown in panel (a) and (b). Both conformations show that this anomer does not fit well into the active side. The spatial distance does hence not allow a reduction. In panel (c) fitting of α-xylose is shown, which matches well into the reactive site close to NADH. The spatial closeness between enzyme and substrate are in good agreement with the STD effects shown in Table 1.

## Mechanism of xylose ring opening to provide reducible aldehyde form

Ring opening prior to binding can be excluded, as both anomers would be accepted equally. However, for reduction the open chain aldehyde form is necessary. The molecular docking provides a fitting of the α-xylose, which is a good starting point for the ring opening. The proton of hydroxyl group in Tyr-51 is in about 2.8 Å distance to the ring oxygen of α-xylose. Hence, it can initiate the opening procedure as shown in Fig. 5(a). The resulting free hydroxylate function of Tyr-51 can be stabilized by the surrounding amino acids or might be protonated from the close Asp-50. The xylose ring opening is then finished by the terminal aldehyde formation and release of the hydroxy proton of position 1. This can be accepted by one of the nearby amino acids, especially the Tyr-51, which might return the proton back to Asp-50. Resulting aldehyde function is close (*ca.* 1.8 Å) to the transferrable pro-*R* hydrogen of NADH (Fig. 5(b)). It is quite likely directly reduced by NADH to xylitol. A slightly different orientation of the aldehyde, however, allows a better fitting (Fig. 5(c)) and still enables the pro-*R* hydrogen transfer.[21,31]

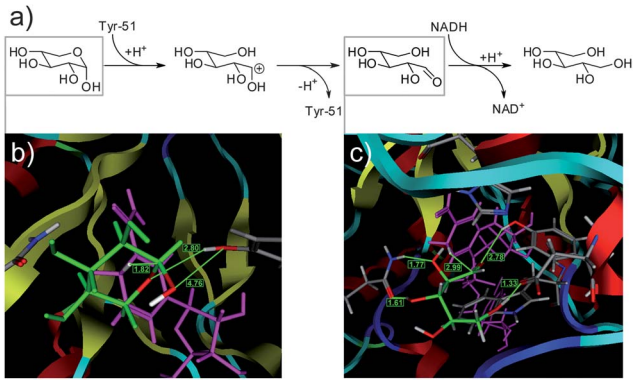


**Fig. 5** Mechanism of xylose ring opening and reduction in the *Ct*XR active side (panel (a)). The distance between the OH-proton of Tyr-51 and the ring oxygen (*ca.* 2.8 Å) is close enough to initiate the ring opening by protonation indicated in panel (b). Although the distance between the oxygens of position 1 and Tyr-51 is reasonable large (4.76 Å) the proton released from position 1 probably re-protonates the Tyr-51 hydroxyl function. The resulting $sp^2$ carbon of the aldehyde is then placed very close to the transferrable pro-*R* hydrogen of NADH (*ca.* 1.8 Å). In panel (c) an optimized fit of the open chain aldehyde prior to hydride transfer is shown.

## STD NMR of the 2,4-dichloroacetophenone/NADH/*Ct*XR complex

Various structures of unnatural substrates, which are reduced by the *Ct*XR with excellent catalytic efficiencies, often differ entirely from those of aldohexoses. In particular, the carbonyl functions of these compounds do not form half acetals or half ketals in aqueous solutions. Their binding in the productive mode is hence entirely different from those of the monosaccharides.

Here, we use 2,4-dichloroacetophenone as a model compound to study binding of aromatic ketones. It is reduced with a high catalytic efficiency of 1128 $s^{-1}$ $M^{-1}$, which has been shown to be caused by an intense polarization of the carbonyl group (Scheme 1).[23] STD NMR recorded from the binary mixture of model substrate (1.5 mM) and enzyme (0.51 μM) shows that the three protons of the terminal methyl group provide the most intense signal. Proton at position 3′ has a comparable STD effect. In contrary the protons H-6′ and, in particular, H-5′ in the aromatic moiety have smaller STD effects, as shown in Table 2. Start of the reaction by addition of the coenzyme lead to formation of the ternary complex and to entire changes in the STD effects. Signal intensity of H-3′ in the substrate increases by a factor of 1.33 and signal of H-5′ reaches the intensity of H-6′. However, the more interesting signals emerge from the resulting alcohol (Scheme 1), which is released from the ternary complex

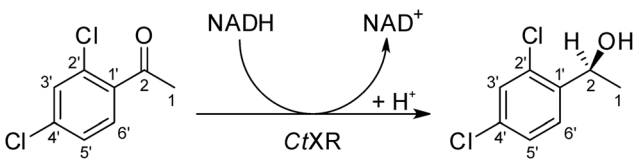


**Scheme 1** *Ct*XR catalyzed reduction of 2,4-dichloroacetophenone to the corresponding (*S*)-1-(2′,4′-dichlorophenyl)-ethan-1-ol. Indication of positions is used in Table 2.

**Table 2** STD NMR effects of 2,4-dichloroacetophenone binding to *Ct*XR in binary and in ternary complex with NADH as well as 1-(2′,4′-dichlorophenyl)-ethan-1-ol binding to *Ct*XR in ternary complex with NADH (generated $NAD^+$) directly released after transformation. The latter two are determined from one measurement. Signal to noise ratio was about 15 in both spectra

| Substrate | H-1[b] | H-2 | H-3′ | H-5′ | H-6′ |
|---|---|---|---|---|---|
| 2,4-Dichloroacetophenone | 100 | — | 30 | −10[a] | 20 |
| 2,4-Dichloroacetophenone/NADH | 100 | — | 40 | 30 | 30 |
| 1-(2′,4′-Dichlorophenyl)-ethan-1-ol/NADH | 20 | 70 | 30 | 40 | 60 |

[a] Phase error are likely caused by an effect discussed earlier and based on interference with $D_2O$ irradiated by the lock frequence.[14] [b] Value refers to all three proton of the methyl group.

for the first time. Here STD effects of protons in positions 2, 5′, and 6′ are distinctly higher than those of the three methyl protons (Table 2). This result shows that 2,4-dichloroacetophenone binding in the binary and ternary complexes differ from each other and that the mode of binding changes entirely during the reduction. However, the experiment also shows that *ca.* 1/4 of the bound 2,4-dichloroacetophenone is released in the unreduced form, indicated by the presence of 2,4-dichloroacetophenone STD signals. The intensity of these signals can be roughly compared, as the binding time of substrate and product are approximately in the same range. The reason for the release is likely a not best possible fit of the unnatural substrate into the active site, which can lead to elevated $k_{off}$ rates.

## Docking simulation of 2,4-dichloroacetophenone/NADH/*Ct*XR complex

The *in silico* molecular docking has been performed for the unnatural model substrate to compare 2,4-dichloroacetophenone/*Ct*XR binding with Xyl/*Ct*XR binding. For this purpose the substrate was changed to 2,4-dichloroacetophenone, while all other parameter remained unchanged. Results indicate that the model substrate does not fit as good as α-xylose and that it can be located in the active site in two different orientations (Fig. 6). In these two cases the hydride would be transferred to the pro-*R* or pro-*S* side of the ketone, respectively, resulting in both enantiomers of the produced alcohol. In both orientations the distance between the transferred hydride and the carbonylic carbon is determined to be about 2.8 Å, which is just close enough to perform the reduction. However, it is known that only the *S*-configured alcohols are formed within *Ct*XR catalyzed reduction of acetophenones.[23,27] Hence, the two different orientations must cause slight variations in activation energy, which cannot be determined accurately by the applied *in silico* molecular docking method. The orientation leading to the *S*-alcohol is productive and causes the hydride transfer, while the other one is not productive and leads to reorientation or to release of the 2,4-dichloroacetophenone. This result comes along with the observed effect of the STD NMR where the unnatural substrate shows relatively high signals compared with those of by far completely transformed α-xylose.

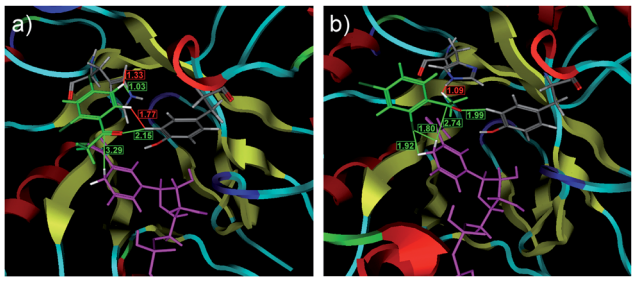


**Fig. 6** Molecular docking of 2,4-dichloroacetophenone to the complex of NADH and *Ct*XR.[18] The substrate and NADH are visualized in green and pink, respectively. Shown are two different orientations (a and b) possessing very similar distances between the transferred hydride and the carbon of the carbonyl group. A couple of indicative distances between atoms are shown in red ($^1$H–$^1$H distances, responsible for STD effects) and green (indicative distances between xylose, NADH, and *Ct*XR). All are indicated with the length given in Å. However, only the orientation shown in panel (a) represents the position of the substrate during hydride transformation, which leads to the solely isolated product (*S*)-1-(2′,4′-dichlorophenyl)-ethan-1-ol by transfer of the pro-*R* hydrogen from NADH.

The results from the molecular docking method have also to be handled with care, because the flexibility of the loop regions in the active site was not taken into account. For a more detailed analysis a molecular dynamic calculation can be helpful. Such investigation may allow to determine the slight differences in activation energy between the two orientations of 2,4-dichloroacetophenone in the active site.

## Conclusions

Reduction of natural and unnatural substrates by *Ct*XR has been studied to certain detail, but was mainly discussed in the context of substrate structures and carbonyl group polarization.[23] However, substrate binding in the ternary complexes also has an important influence on the catalytic efficiency. Here, two different NMR based methods as well as molecular docking were used to show that transformations of xylose and similar aldoses are initiated by binding of the respective α-anomers. This selective binding and the concomitant broad acceptance of various aldoses for reduction suggests that xylose is not the only natural aldose, which is transformed by *Ct*XR. The preferential binding of α-anomers suggests an opening of the pyranose form to an open chain aldehyde, which is consecutively reduced. Binding studies with both anomers of *O*-methyl-glycosides indicate the preferred binding of α-pyranose form.

Despite the highly flexible substrate binding pocket of *Ct*XR, docking of the very well accepted unnatural 2,4-dichloroacetophenone into a rigid structure of *Ct*XR/NADH illustrates a good fitting. This finding contributes to explain the high catalytic efficiency of the reaction. However, the used molecular docking method cannot clarify the enantioselectivity of the transformation. Hence, better refined molecular dynamic studies are necessary to get a more detailed picture of the ternary complexes, in particular, with respect to the flexible loop region, which is involved in substrate fixation. These applications should allow to predict catalytic efficiencies based on molecular docking as well as on determination of the carbonyl group polarization. Furthermore, results can be used as guideline for a rational enzyme redesign to improve the *Ct*XR-catalyzed reduction of unnatural substrates in order to allow an optimized application in the synthesis of pharmaceuticals.[27]

## Experimental

### Chemicals

All chemical used were purchased from Sigma-Aldrich-Fluka (Taufkirchen, Germany) or Carbosynth (Berkshire, UK) with the highest purity available and used without further purification or drying.

### NMR spectroscopy

Samples were prepared in 0.7 mL $D_2O$ and contain ~1.0–20.0 μL of the *Ct*XR (13 mg mL$^{-1}$) in 50 mM potassium phosphate buffer solution at a pD-value of 6.6.[32] The respective substrates concentrations are reported for each experiment. Amounts of *Ct*XR are indicated for the experiments in the results part. Due to low solubility, the 2,4-dichloroacetophenone was dissolved in 0.07 mL $CD_3OD$ first and then added to the sample. All $^1$H and STD NMR spectra were measured on a Bruker (Rheinstetten, Germany) DRX-600 AVANCE spectrometer at 600.13 MHz using triple resonance 5 mm inverse probe. Measurement temperature was 303 K, or 283 K for some indicated *in situ* NMR measurements. Anomeric mixtures of Xyl, Glc, or Gal used for the *in situ* NMR measurements were equilibrated for 10 days at the measurement temperature until no more anomerisation was detectable by $^1$H NMR. All chemical shifts were referenced to external acetone at 2.225 ppm.

### STD NMR

STD NMR spectra were recorded as described earlier.[15] The molar substrate–*Ct*XR and cosubstrate–*Ct*XR ratios were in the range between 2 900 : 1 and 14 700 : 1. Substrate and cosubstrate concentrations were between 1.5 mM to 7.5 mM. Selective saturation of the protein was achieved by a series of 40 Gaussian pulses of 50 ms length, and 1 ms delay resulting in a total irradiation times of 2.04 s. On resonance measurements were performed at −2.0 ppm and off resonance at 40.0 ppm. Subtraction of the spectra was performed during the measurement *via* phase cycling and concomitant change of the irradiation frequency. No water suppression was used to avoid influences onto intensities of signals close to HDO signal. To eliminate protein frequencies a 30 ms spin lock was added after the 90° pulse.

The number of scans for the experiments varied between 128 and 256. Resulting short measurement times allowed to monitor the reaction progress with changing concentration and enabled STD NMR measurements during the transformations. Only measurements with the same parameters have been compared, when different complexes have been studied and matched. For the interpretation the largest signal in all comparable experiments was set to 100% and the relative intensities were determined in steps of 10%.[14,15]

### *In situ* NMR

For *in situ* NMR between 16 and 64 proton measurements were performed in regular intervals over a total time of 3–8 h. Each spectrum was recorded with 64 scans.[16,17]

### Computational methods

For the molecular docking calculations the X-ray structure of the *Ct*XR [1MI3 from the RCSB PDB] is used and further more optimized. For that purpose a monomer is cut off the tetrameric enzyme and the $NAD^+$ is changed to NADH. Additionally a structure optimization is performed after adding the hydrogens, which are needed to determine proton–proton distances. The docking calculations were performed using MOE program version 2008.10 (Molecular Operating Environment, http://www.chemcomp.com) with this refined structure. The used settings are for the placement: triangle matcher with default configuration. Refinement is done by Forcefield with default configurations and retain is set to 100. Docking is performed as 'free' docking as well as constraining the docking to the binding side (NADH, Asp-50, Tyr-51, His-113,…). All these calculations are made three times with default settings. Also redock calculations were done with the best fitted molecule structures to provide local minima.

## Acknowledgements

We thank Prof. Dr Peter Wolschann for kind help with docking simulation and Ing. Susanne Felsinger for measuring NMR spectra. We are grateful to Prof. Dr. B. Nidetzky and Dr Regina Kratzer (both TU Graz) for providing the *Ct*XR and for valuable discussions.

## Notes and references

1 K. Nakamura, R. Yamanaka, T. Matsuda and T. Harada, *Tetrahedron: Asymmetry*, 2003, **14**, 2659.
2 S. W. May, *Curr. Opin. Biotechnol.*, 1999, **10**, 370.
3 J. D. Stewart, *Curr. Chem. Biol.*, 2001, **5**, 120.
4 K. Hoelsch and D. Weuster-Botz, *Enzyme Microb. Technol.*, 2010, **47**, 228.
5 X. Q. Mu, Y. Xu, M. Yang and Z. H. Sun, *Process Biochem.*, 2011, **46**, 233.
6 R. Devaux-Basseguy, A. Bergel and M. Comtat, *Enzyme Microb. Technol.*, 1997, **20**, 248.
7 D. Giacomini, P. Galletti, A. Quintavalla, G. Gucciardo and F. Paradidi, *Chem. Commun.*, 2007, 4038.
8 R. Kratzer and B. Nidetzky, *Chem. Commun.*, 2007, 1047.
9 A. Gutteridge and J. Thornton, *FEBS Lett.*, 2004, **567**, 67.
10 V. K. Pliska, in *Handbook of Proteins*, ed. M. M. Cox and G. N. Phillips, Wiley-VCH, Weinheim, 2007, vol. 1, p. 417.
11 B. Meyer and T. Peters, *Angew. Chem., Int. Ed.*, 2003, **42**, 864.
12 J. Angulo and P. M. Nieto, *Eur. Biophys. J.*, 2011, **40**, 1357.
13 M. Mayer and B. Meyer, *Angew. Chem., Int. Ed.*, 1999, **38**, 1784.
14 L. Brecker, A. Schwarz, C. Gödl, R. Kratzer, C. E. Tyl and B. Nidetzky, *Carbohydr. Res.*, 2008, **343**, 2153.
15 L. Brecker, G. D. Straganz, C. E. Tyl, W. Steiner and B. Nidetzky, *J. Mol. Catal. B: Enzym.*, 2006, **42**, 85.
16 L. Brecker and D. W. Ribbons, *Trends Biotechnol.*, 2000, **18**, 197.
17 J.-P. Grivet, A.-M. Delort and J.-C. Portais, *Biochimie*, 2003, **85**, 823.
18 Y. Yuan, X. Wen, A. R. D. Sanders and B. M. Pinto, *Biochemistry*, 2005, **44**, 14080.
19 W. Neuhauser, D. Haltrich, K. D. Kulbe and B. Nidetzky, *Biochem. J.*, 1997, **326**, 683.
20 P. Mayr, K. Brueggler, K. D. Kulbe and B. Nidetzky, *J. Chromatogr., B: Biomed. Sci. Appl.*, 2000, **737**, 195.
21 R. Kratzer, S. Leitgeb, K. D. Wilson and B. Nidetzky, *Biochem. J.*, 2006, **393**, 51.
22 R. Kratzer, M. Purkl, S. Egger, M. Vogl, L. Brecker and B. Nidetzky, *Biotechnol. Bioeng.*, 2011, **108**, 797.
23 M. Vogl, R. Kratzer, B. Nidetzky and L. Brecker, *Org. Biomol. Chem.*, 2011, **9**, 5863.
24 W. Neuhauser, D. Haltrich, K. D. Kulbe and B. Nidetzky, *Biochemistry*, 1998, **37**, 1116.
25 T. Ikeda and M. Senda, *Bull. Chem. Soc. Jpn.*, 1973, **46**, 1650.
26 P. Delahay and J. E. Strassner, *J. Am. Chem. Soc.*, 1952, **74**, 893.
27 M. Vogl, R. Kratzer, B. Nidetzky and L. Brecker, *Chirality*, 2012, **24**, 847.
28 N. R. Krishna and V. Jayalakshmi, *Top. Curr. Chem.*, 2008, **273**, 15.
29 A. Bhunia, S. Bhattacharjya and S. Chatterjee, *Drug Discovery Today*, 2012, **17**, 505.
30 B. Morawski, G. Casy, C. Illaszewicz, H. Griengl and D. W. Ribbons, *J. Bacteriol.*, 1997, **179**, 4023.
31 L. K. Kananagh, M. Klimacek, B. Nidetzky and D. K. Wilson, *Biochemistry*, 2002, **41**, 8785.
32 pH values were calculated according to: pD = pH + 0.4. P. R. Mussini, T. Mussini and S. Rondinini, *Pure Appl. Chem.*, 1997, **69**, 1007.

 